Anal Bioanal Chem (2009) 393:1091–1105
DOI 10.1007/s00216-008-2410-4

REVIEW

Delivering quantum dots into cells: strategies, progress and remaining issues

James B. Delehanty · Hedi Mattoussi · Igor L. Medintz

Received: 4 July 2008 / Revised: 15 August 2008 / Accepted: 12 September 2008 / Published online: 5 October 2008

Abstract The use of semiconductor quantum dots (QDs) in biological sensing and labeling continues to grow with each year. Current and projected applications include use as fluorescent labels for cellular labeling, intracellular sensors, deep-tissue and tumor imaging agents, sensitizers for photodynamic therapy, and more recently interest has been sparked in using them as vectors for studying nanoparticle-mediated drug delivery. Many of these applications will ultimately require the QDs to undergo targeted intracellular delivery, not only to specific cells, but also to a variety of subcellular compartments and organelles. It is apparent that this issue will be critical in determining the efficacy of using QDs, and indeed a variety of other nanoparticles, for these types of applications. In this review, we provide an overview of the current methods for delivering QDs into cells. Methods that are covered include facilitated techniques such as those that utilize specific peptide sequences or polymer delivery reagents and active methods such as electroporation and microinjection. We critically examine the benefits and liabilities of each strategy and illustrate them with selected examples from the literature. Several important related issues such as QD size and surface coating, methods for QD biofunctionalization, cellular physiology and toxicity are also discussed. Finally, we conclude by providing a perspective of how this field can be expected to develop in the future.

Keywords Semiconductor quantum dot · Peptide · Nanoparticle · Endocytosis · Electroporation · Biosensor · Cellular labeling · Microinjection · Transfection · Polymer · Fluorescence

J. B. Delehanty · I. L. Medintz (✉)
Center for Bio/Molecular Science and Engineering,
Code 6900, U. S. Naval Research Laboratory,
Washington, DC, USA
e-mail: igor.medintz@nrl.navy.mil

H. Mattoussi
Division of Optical Sciences, U.S. Naval Research Laboratory,
Code 5611,
Washington, DC 20375, USA

Introduction

Among an array of potential nanoparticle materials currently being developed for use in biology (for example those made from noble metals, transition metals, silicon and functionalized polymers), luminescent semiconductor nanocrystals or quantum dots (QDs) provide unique intrinsic photophysical properties for potential medical, diagnostic and basic research applications. QDs have high quantum yields and high molar extinction coefficients (~10–100× those of organic dyes) along with exceptional resistance to both chemical and photodegradation. Two spectrophotometric properties are of particular interest: the ability to size-tune the narrow symmetrical emissions (full width at half maximum ~25–40 nm) as a function of core size [1], and the broad excitation spectra which increase continuously towards the UV [2–6]. This also allows the excitation of multiple mixed or differentially emissive QD populations (multiplexing) at one wavelength far removed from their individual emissions (large effective Stoke's shift), a feature that cannot be achieved with conventional fluorophores; see Fig. 1. Further, QDs have very high two-photon action cross-sections; these are typically almost two orders of magnitude larger than currently utilized organic dye molecules (10,000–20,000 GM units at 800 nm) [7, 8]. This allows access to an ideal tissue optical transparency

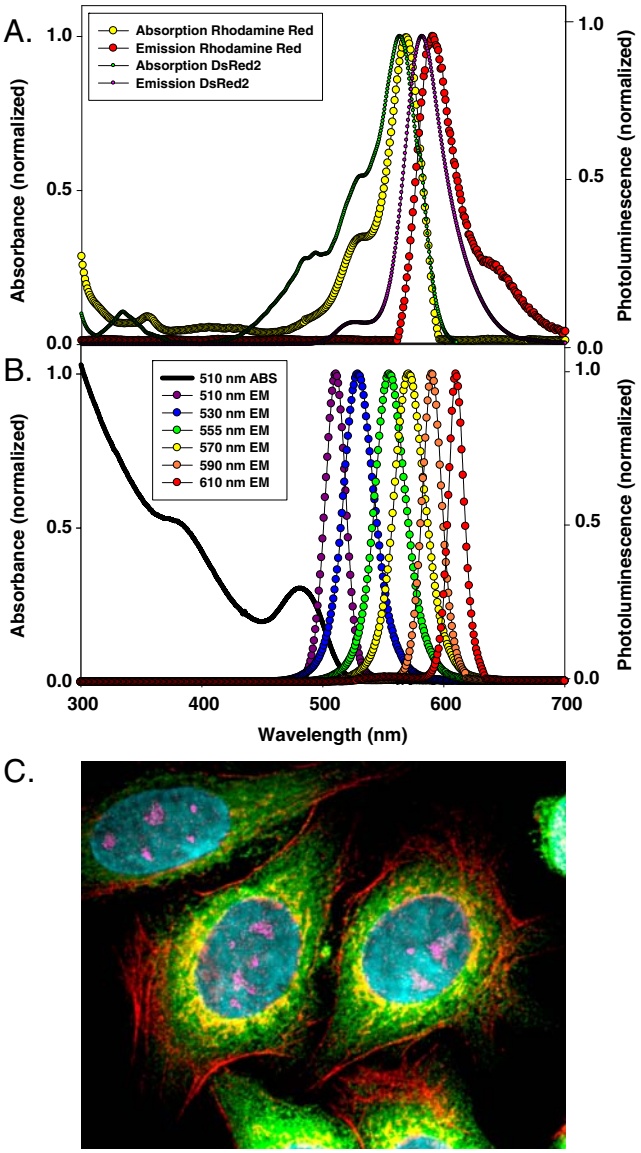

Fig. 1 Semiconductor quantum dot fluorescent properties. Comparison of rhodamine red/DsRed2 spectral properties to those of QDs, highlighting how multiple narrow, symmetric QD emissions can be used in the same spectral window as that of an organic or genetically encoded dye. **A** Absorption (*Abs*) and emission (*Em*) of rhodamine red, a common organic dye and genetically encoded DsRed2 protein. **B** Absorption and emission of six different QD dispersions. The *black line* shows the absorption of the 510-nm emitting QDs. Note that at the wavelength of lowest absorption for the 510-nm QD, ~450 nm, the molar extinction coefficient is greater than that of rhodamine red at its absorption maximum (~150,000 vs. 129,000 $M^{-1}cm^{-1}$). **C** Pseudocolored image depicting five-color QD staining of fixed human epithelial cells. *Cyan* corresponds to 655-nm QDs labeling the nucleus, *magenta* to 605-QDs labeling Ki-67 protein, *orange* to 525-QDs labeling mitochondria, *green* to 565-QDs labeling microtubules, and *red* to 705-QDs labeling actin filaments. Adapted with the permission of Macmillan Publishers Ltd. (Nature Materials) [2], copyright 2005

window for multiphoton excitation and low background monitoring. QDs have also been shown to be excellent fluorescence resonance energy transfer (FRET) donors with an array of dye-labeled sensing molecules attached to their surface [9–12].

QDs are typically synthesized from a variety of semiconductor materials which can provide access to a full range of potential emission wavelengths and are utilized as either core-only or core–shell structures (see Table 1 for a list of representative materials). Core–shell nanoparticles are more desirable for biological applications as the shell (usually a wider band-gap material) passivates the core, improves fluorescent properties and prevents leaching [2–6]. High-quality QDs are most commonly synthesized in organic solution and surface-stabilized with hydrophobic organic ligands and thus lack intrinsic aqueous solubility. Biological applications require the further modification of the QD surface with a variety of bifunctional surface ligands or caps to promote solubility in aqueous media [2, 6]. The two principal strategies for accomplishing this have been either wholesale cap-exchange of the native ligand or interdigitation of the native coordinating ligand with a variety of amphiphilic polymers. For cellular imaging and many other biological applications, the attachment of biological molecules (for example, antibodies, proteins, peptides, DNA) to the QD surface is necessary to provide the desired specific biorecognition and/or targeting. In some cases, the QD surface ligands can provide unique functional groups, such as carboxyls or amines, for the multistep covalent chemical coupling of biomolecules [2, 6, 13]. Alternatively, QDs can be directly cap-exchanged with thiolated molecules such as peptides [14] or allowed to interact with appropriately modified peptides or proteins that can coordinate to their surface via metal-affinity interactions [10, 15]. Commercial QD materials are also available that are conjugated to streptavidin or specific antibody binding proteins such as protein G [2, 16, 17]. The interested reader is referred to several pertinent reviews that discuss many of these issues in detail [3–6, 10].

Table 1 Photophysical characteristics of representative quantum dots[a]

Core(shell) materials	Core diameter size range (nm)	Typical emission range (nm)
ZnS	0.7–2.1	300–400
ZnSe	2.0–5.0	325–450
CdS	2.8–5.3	375–475
CdSe(ZnS)	2.0–8.0	480–650
CdTe	3.2–9.0	540–750
CdTe(CdSe)	4.0–9.4	640–860
InP	2.6–4.5	625–720
InAs	3.4–6.0	860–1250

[a] Compiled from [1–3, 81] and references therein

Intracellular potential of quantum dots

QDs have already been shown to be effective fluorophores for simultaneously visualizing multiple proteins and nucleic acids in fixed tissues and cells (see Fig. 1C for a 5-QD color staining example) and for polychromatic extracellular membrane labeling with up to eight QD colors in flow cytometric analysis [3–6, 10, 16, 18]. However, it is specifically in the areas of in vivo imaging, intracellular labeling and even some clinical applications that QDs hold the most promise. For almost all of these applications, the ability to achieve intracellular delivery will be a key issue; see Table 2 for a partial list of selected applications in this context. The projected utility here includes fluorescent labels for intracellular imaging of multiple cellular targets, contrast agents for the visualization of targeted tissues and cells such as tumors, nanoscale platforms for in vivo sensors, and more recently the role of delivery vehicles for drugs has also been proposed [19–24]. As compared to the currently available chemical-based technologies, QDs are generating interest in these areas due to the unique combination of physiochemical properties their nanoscale size provides.

In vivo, their relatively small size can allow the penetration of capillaries and even the targeting of subcellular organelles [21, 22, 24]. Their intrinsic fluorescence can be exploited for a particular fluorescent application, i.e., deep-tissue imaging [25], or alternatively these properties could be combined with another material such as ferric oxide nanoparticles to yield multimodal fluorescent/magnetic resonance contrast probes in one vector [25–27]. Their high surface-to-volume ratios can also provide for the attachment of multiple different chemicals/biological molecules, each of which can provide a separate desired function [3]. For example, a tumor-targeting QD can be functionalized with a combination of tumor-recognition antibodies for both specific binding and in vivo fluorescent localization, drugs for therapy, and radiolabels for imaging or radiation dosing [3, 21, 24]. Further, the ability to attach multiple such moieties to a single nanoparticle can serve to increase binding affinity, avidity and drug dosage potency [24]. QDs may also uniquely enhance in vivo photodynamic therapy (PDT) therapy [27]. Conventional PDT agents are poorly soluble and are hard to target and excite once administered in vivo. The QDs can act as nanoscaffolds and solubilizers for the attachment of a high ratio of PDT agents along with anticancer targeting antibodies. They can also function as "energy-harvesting antenna" for PDT therapy due to their large one- and two-photon absorption cross-sections. These properties allow them to be both efficiently excited even deep within tissues and to sensitize proximal PDT agents via energy transfer [27]. Before realizing all of these applications, however, the first and perhaps most significant hurdle that must be overcome is the development of facile methods for targeted intracellular delivery of both QDs and QD bioconjugates.

Table 2 Selected applications of biocompatible quantum dots where cellular delivery is key to the subsequent function

Application	References
Monitoring cellular receptor trafficking	[46]
Monitoring intracellular trafficking	[61, 66]
Evaluating cancer cell metastic potential	[90]
Multicolor cellular labeling for tracking	[95]
Vital cellular labeling	[16, 29, 30, 82]
In vivo imaging	[7]
Tumor imaging	[96, 97]
Monitoring cellular movement	[98]
Monitoring membrane dynamics	[99]
Nanoparticle-mediated drug delivery	[20]
Monitoring cellular fate during development	[67, 68]

Intracellular delivery of quantum dots

The methods employed to date for the intracellular delivery of QDs, and a variety of other nanoparticles, can be grouped into derivatives of three strategies which are loosely based on their intrinsic physiochemical nature.

I. *Passive delivery*, which relies on the inherent physicochemical properties of the QD itself (surface functionalization and charge) to mediate cellular internalization.
II. *Facilitated delivery*, which typically involves decorating the QD surface with a functional molecule that can be biological in nature (such as a peptide or protein) or other functional chemicals such as polymers or drugs. These allow QD intracellular uptake via endocytosis, a constitutive cellular process whereby cells take up extracellular material (proteins, nutrients, cofactors, etc.) from the surrounding environment by engulfing it within their cell membrane and forming a vesicle that is subsequently transported to the cytoplasm [28]. The (bio)molecules attached to the QD's surface facilitate the initial QD conjugate–cell membrane interaction.
III. *Active delivery*, which involves direct manipulation of the cell, and this includes physical techniques such as microinjection and electroporation.

Specific examples are used below to highlight how each strategy has been applied, and additional examples are listed in Table 3.

Some of the intrinsic differences in the delivery mechanisms themselves give rise to concomitant differences in the resulting pattern of QD cellular labeling. Endocytosis often results in QD sequestration within endocytic vesicles and leads to a generalized punctate or "spotty" fluorescence staining pattern (see Fig. 2A). Other

Table 3 Selected methods utilized for the intracellular delivery of quantum dots

Strategy	Mechanism	Examples	Targeted Cells	References
Passive uptake (nonspecific)	Electrostatic interactions		HeLa, human macrophages	[29, 32]
			Human mammary epithelial tumor (MDA-MB-231)	[98, 100]
Facilitated delivery	Peptide-mediated	TAT	Human embryonic kidney (HEK), HeLa, mesenchymal stem cells, Jurkat cells	[13, 30, 36–40, 69, 82, 101]
		Pep-1 (Chariot)	Osteoblast, vascular endothelial cells	[42]
		RGD motif	Fibroblast (NIH 3T3), epidermoid carcinoma	[43, 44]
		Neuropeptide	HeLa	[45]
		Polylysine		[83, 84
	Protein-mediated	Transferrin	Human pancreatic cancer	[49, 50, 52–54]
		Antibody	Breast cancer (MCF-7), mesenchymal stem cells	[51, 55, 85]
		EGF	Chinese hamster ovary	[46–48]
		Cholera toxin B	Fibroblast	[56, 86]
		NGF	PC12 neural cells	[87, 88]
	Polymer/lipid-mediated	Lipid polymers	Mouse lymphoma, HeLa, HEK293, A549 epithelial lung HeLa	[57–60, 89, 90]
		Polyethyleneimine	HeLa	[61]
		Cholesterol		[91]
	Drug-mediated	Tiopronin	Fibroblast	[92]
	Small molecule	Glucose/sugar	*S. cerevisiae* (Baker's yeast)	[62, 102]
		Folate	Epidermal carcinoma	[63]
		Adenine/AMP	Bacteria (*Bacillus subtilis*, *E. coli*)	[93]
		Dopamine	A9 mouse fibroblast with transfected dopamine receptor	[94]
Active Delivery	Electroporation		HeLa, mouse neural stem progenitor cells	[58, 66]
	Microinjection		Xenopus embryo, HeLa, COS-1 African green monkey kidney, human embryonic kidney	[58, 68, 82]

polymer-based techniques result in fluorescent labeling similar to endocytosis with a subtle distribution of QD fluorescence to various subcellular organelles and compartments (see Fig. 2B for an example of perinuclear staining). Lastly, physical methods such as direct microinjection into the cytoplasm can result in a more homogeneous labeling of the cytoplasm while excluding the nuclear compartment (see Fig. 2C).

Passive delivery

The term "passive delivery" can be slightly misleading, as uptake in this case still relies on cellular endocytosis; it is actually used to indicate that beyond being made hydrophilic, the QD surface is not functionalized any further, and initial cellular interactions rely on "passive" membrane–QD interactions, which are essentially electrostatic in nature.

Electrostatic interactions In one of the first prominent demonstrations of the use of passive uptake for QD delivery, Jaiswal et al. incubated HeLa cells with negatively charged DHLA-capped CdSe/ZnS QDs at concentrations of 400–600 nM for 2–3 h and showed that the cells internalized the materials via nonspecific endocytosis and that the QDs ultimately remained sequestered within endosomal compartments, even after several days in culture; see Fig. 3A [29]. While a high degree of uptake was noted, rather high concentrations of QDs were required with longer incubation times than some of our later results achieved with QD-TAT peptide bioconjugates, as discussed below [30]. This difference in concentration and time essentially reflects the strong membrane avidity provided by the TAT peptide and how it can facilitate rapid endocytic uptake. Jaiswal also showed that common slime mold/social amoeba cells (*Dictyostelium discoideum*) could also take up QDs in the same manner and still develop normally and respond to cAMP signaling when starved. LeDuc's group was able to build upon these latter findings and utilize passive uptake to deliver 655 nm QD phalloidin conjugates to the same cells [31]. This allowed them to specifically monitor the spaciotemporal rearrangements of the cytoskeletal actin filaments within the mold cells during cell motility. In a recent study, Nabiev et al. used CdTe QDs capped with thioglycolic acid to monitor the passive uptake of different-sized nanocrystals (2–6 nm) by cell lines of different morphological lineages including macrophages, phagocytic, epithelial and endothelial cells [32]. Interestingly, they observed that the intracellular distribution of the QDs varied in accord with particle size; smaller, green-emitting QDs (~2 nm in diameter) preferentially located to the nucleus, while larger, red-emitting QDs (~6 nm

diameter) remained in the cytoplasm; see Fig. 3B. The authors cited the reversible protonation of the thioglycolic acid capping ligands within the acidic endolysosomal compartment as the putative mechanism by which the QDs are able to escape endosomal sequestration.

The main advantage of passive delivery is simplicity; it does not require the further functionalization of the QD surface with a targeting ligand for uptake. QDs are simply incubated with the cells at the appropriate concentration and exposure time and they are subsequently internalized by nonspecific endocytosis. Similar to facilitated delivery and electroporation (below), QDs can be delivered to large numbers of cells at once. However, this technique is not tailored to a specific cell type and endosomal escape will remain an impediment to the delivery of the QD to the cytoplasm or other organelles. Furthermore, incubating cells with high concentrations of QDs and for long periods of time can enhance cytotoxicity in some cases [33].

Facilitated delivery

Peptide-mediated uptake

For this strategy, a peptide sequence (MW <3 kD) is used to facilitate cellular uptake by endocytosis, and it provides the initial interaction with a cellular membrane receptor or alternatively a more generalized electrostatic interaction [34]. This is also the key initial event that allows the QD conjugate to exploit and undergo subsequent uptake by cellular endocytosis. Four commonly used peptide sequences are reviewed below.

TAT The use of the TAT peptide motif derived from the HIV-1 virus TAT protein has proven to be a popular and powerful means by which to deliver a variety of cargos to cells [35]. When coupled to the QD surface, the arginine- and/or lysine-rich TAT peptide (usually a linear Arg_{8-10} repeat) presents a highly positively-charged ligand that interacts with negatively charged receptors on the cell surface (e.g., heparan sulfate proteoglycans). We have showed that a TAT-based Arg_8 peptide could be non-covalently self-assembled onto the surface of CdSe/ZnS QDs surface-capped with dihydrolipoic acid (DHLA) via metal-affinity coordination between a polyhistidine tract present at the peptide's terminus and the QD surface Zn atoms [15, 30]. Peptide-functionalized QDs were internal-

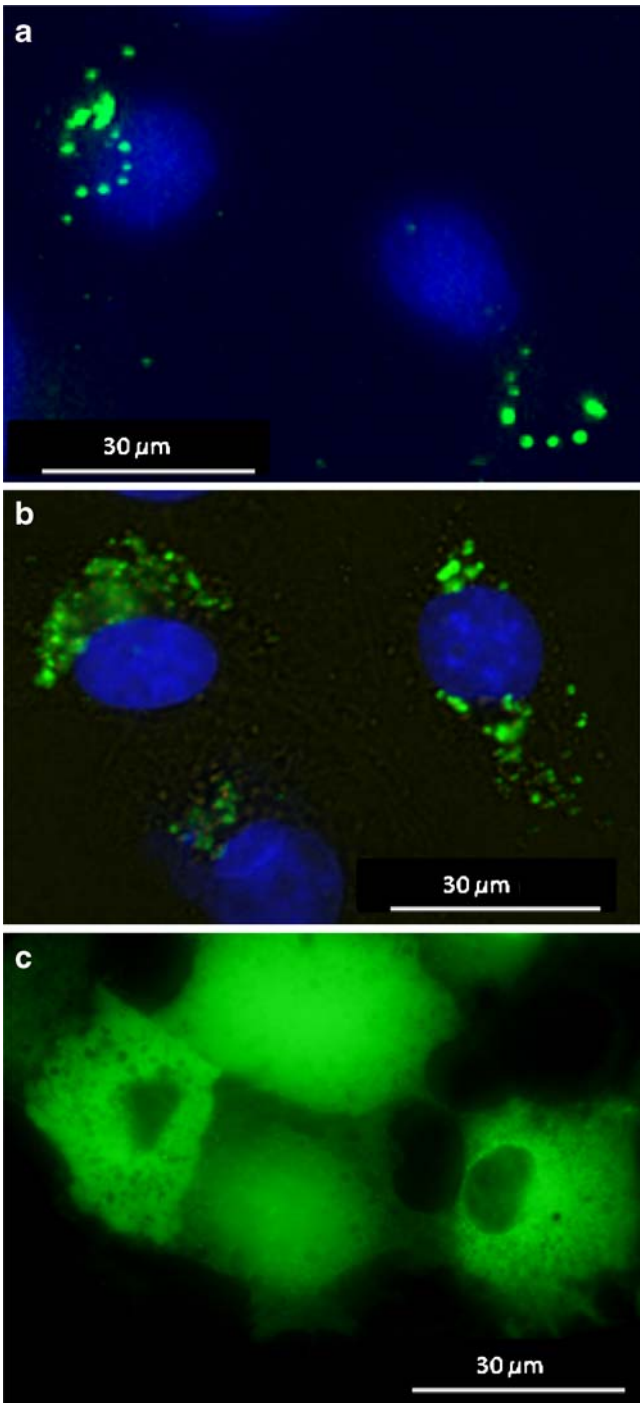

Fig. 2 Cellular staining patterns. COS-1 cells subjected to different QD delivery strategies. **A** Cells exposed to dihydrolipoic acid (DHLA)-modified QDs (*green*) functionalized with TAT cell penetrating peptide for 1 h, which results in the characteristic punctuate appearance of endosomal sequestration. Cells were counterstained with DAPI (*blue*) to visualize the nuclei. Figure reproduced from [30] with the permission of the ACS. **B** Mixed surface DHLA/PEG QDs complexed with the commercial polymer Pulsin that have been exposed to cells for several hours and observed after five days of culture. A slightly diffuse perinuclear staining pattern is observed in this case. **C** Cells 15 min post-microinjection with PEG-functionalized QDs using an Eppendorf InjectMan® NI2 micromanipulator equipped with a FemtoJet programmable microinjector. Direct access to the cytoplasm results in an almost complete/uniform staining pattern, leaving the nuclei clearly visible and outlined

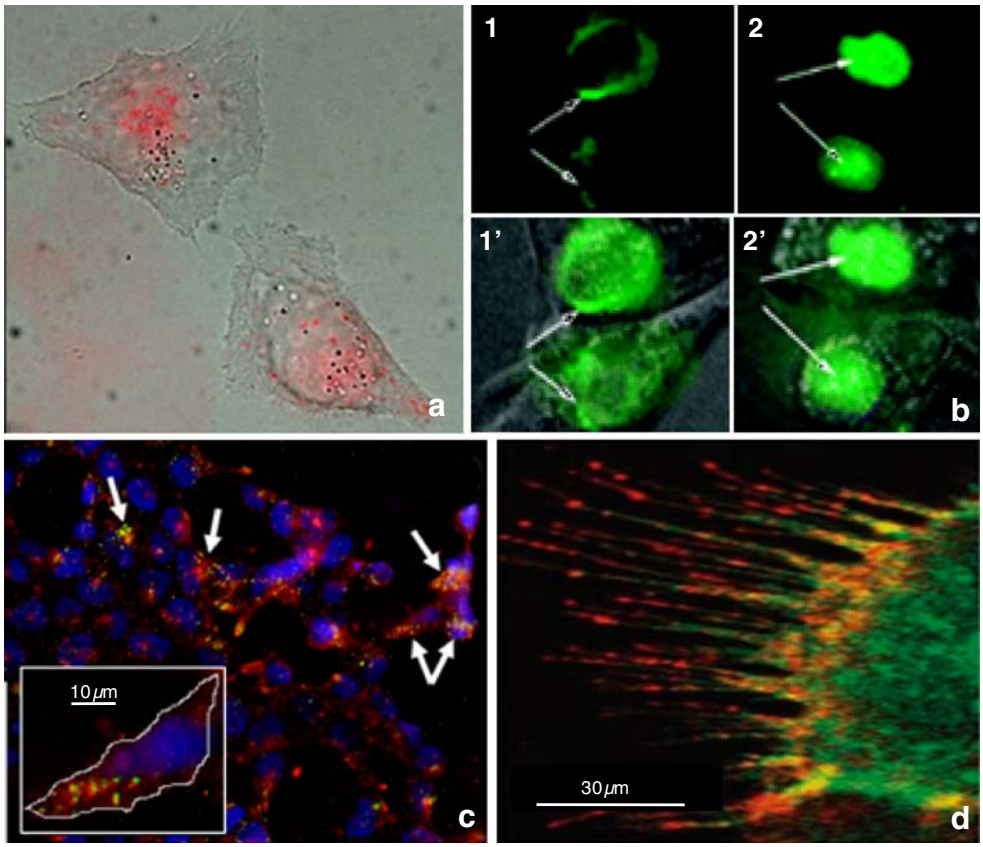

Fig. 3 Passive delivery and peptide- or protein-mediated QD uptake. **A** Passive delivery. A fluorescence/phase image of HeLa cells that were incubated with orange QDs for 2 h followed by removal and washing. The cells shown were imaged 1 day after incubation with QDs. Adapted with the permission of Macmillan Publishers Ltd. (Nature Biotechnology) [29], copyright 2003. **B** Green-emitting CdTe QDs (2.1 nm in diameter) taken up passively by macrophages. After 10 min the QDs were located perinuclearly (*panel 1*), but after an additional 30 min the QDs had accumulated in the nucleus (*panel 2*). *Panels 1′ and 2′* show fluorescence/phase merged images. (Note that the fluorescent intensities in the panels are slightly different.) Figure reproduced from [32] with the permission of the ACS. **C** Peptide-mediated delivery. Human embryonic kidney cells (HEK 293T/17) with green-emitting DHLA QDs delivered as a complex with a TAT-derived peptide. The endocytic compartment was counterlabeled with AlexaFluor-647-conjugated transferrin. The *inset* shows the high degree of colocalization of the QDs within the endosomes of a single outlined cell. Figure reproduced from [30] with the permission of the ACS. **D** Protein-mediated QD delivery. Epidermoid carcinoma A431cells expressing the EGF receptor as a fusion protein with mCitrine (*yellow*) were incubated with red-emitting QDs conjugated to EGF (*red*). The image shows the areas of red QDs merged with yellow mCitrine-fused EGF receptors in *orange*. Adapted with the permission of Macmillan Publishers Ltd. (Nature Biotechnology) [46], copyright 2004

ized via endocytosis (as verified by counterstaining) in both HEK293T/17 and COS-1 cells (Fig. 3C). Internalization was found to be dependent on both the QD concentration and/or the number of peptides assembled onto the QD surface. Examination of QD toxicity showed that in both cell lines the duration of the QD incubation was a key determinant. Incubation of cells with QD-peptide for acute or short one-hour periods (sufficient time to achieve efficient uptake) followed by a twenty-four hour culture resulted in negligible toxicity (less than 10% cell death).

Ruan et al. created a similar conjugate by utilizing a biotinylated form of the native TAT peptide to form a noncovalent QD-peptide assembly with commercial streptavidin-conjugated QDs [36]. When incubated with HeLa cells, the QD bioconjugates were first localized entirely at the plasma membrane, but were ultimately taken up to the cell interior when monitored over a 24-h period. By using a variety of counterstains, the authors observed that the QDs were located in various cellular subcompartments including, predominantly in a perinuclear region known as the microtubule organizing center (MTOC). They also noted that a sizable fraction of the QD-TAT conjugates were associated with the inner leaflet of the membranes of endocytic vesicles and the outer surface of vesicles; the latter were shed from filopodia. In a modification, TAT peptide-mediated cellular uptake was utilized to preload and label stem cells for later in vivo fate determination. Lei et al. covalently attached the native TAT peptide to the endgroups of polyethylene glycol (PEG)-capped CdSe/ZnS QDs to achieve efficient delivery into mesenchymal stem

cells [37]. They subsequently injected the QD-loaded stem cells into the tail veins of SCID (nude) mice and tracked the labeled cells as they localized to the liver, lung and spleen. Several other groups have also utilized the TAT peptide to deliver various types of functionalized QDs to cells, demonstrating the continuing popularity of this approach [38–40]. We have recently shown that this powerful delivery mechanism can also facilitate the specific intracellular uptake of QDs carrying protein cargos that range from several 100 to up to ~1000 kD/QD on average [2, 13].

Pep-1 Another peptide that has proven useful for the intracellular delivery of QDs is Pep-1 (available commercially as Chariot^{TM}). It is based on a short 21-residue amphipathic, membranotropic sequence (KETWWETWWTEWSQPKKKRKV) commonly used as a noncovalent carrier of peptides, proteins and nucleic acids into cells. As opposed to the viral TAT peptide described above, this signaling sequence is completely synthetic in origin [41]. To facilitate interaction with this peptide and utilize it for cellular delivery, the QD surface first needs to be decorated with a protein which acts as an "intermediary linker" between Pep-1 and the QD. It is believed that Pep-1 associates with proteins via its hydrophobic core, which also associates with the cellular membrane, while the lysine-rich region promotes solubility, allowing the QD to be shuttled into the cell as cargo. Using this strategy, Rozenzhak and coworkers were able to efficiently deliver commercial streptavidin-conjugated CdSe/ZnS QDs into Jurkat cells [42]. When they further decorated the streptavidin with a biotinylated nuclear localization peptide (NLS, derived from the Simian virus 40—SV40 large T-antigen), they observed the internalized QDs eventually accumulating in the nucleus. The percentage of cells showing nuclear accumulation of QDs, however, was low (~10%). The authors attributed this inefficient nuclear targeting to the dissociation of the NLS from the QD, as it was not covalently attached to the QD surface. This particular result is intriguing, as many others have noted that QD–peptide conjugates remain entrapped within endolysosomal compartments.

RGD Several researchers have used the specific interaction of the tripeptide arginine-glycine-aspartate (commonly referred to as the "RGD" motif) with heterodimeric cell surface receptors known as integrins to facilitate QD delivery. Lieleg et al. used a biotinylated, cyclic RGD-containing peptide in which the RGD sequence was separated from the biotin moiety by spacers of varying lengths [43]. When the peptide was complexed with streptavidin-functionalized QDs, the authors showed that the efficiency of cellular uptake correlated well with the length of the spacer, as the RGD-binding site is located in a deep cleft between the two integrin subunits on the cell membrane. Smith and coworkers used a cyclic RGD peptide that targeted the QDs specifically to endothelial cells involved in the formation of new blood vessels, as these cells preferentially express integrins on their cell surface [44]. In this case, the labeling allowed specific imaging of tumor blood vessels in living mice, and the authors further showed that the QDs do not extravasate after uptake. They also found rather unexpectedly that the QD conjugates only bind to the target integrins as aggregates and not as individual QD monomers, suggesting the need for higher avidity from multiple interactions for effective binding with these receptors.

Neuropeptide Biju et al. utilized the small insect neuropeptide hormone allatostatin-1 (APSGAQRLYGFGL) to mediate QD uptake by NIH 3T3 and A431 cells [45]. Biotinylated allatostatin-1 was assembled with streptavidin-conjugated QDs and the complexes were incubated with the cells to promote endocytosis. The authors noted that, 1 h after incubation, the QD signal was still localized primarily in the endosomes, while a small portion of the QD signal appeared to be in the cytoplasm associated with microtubules and partially in the nucleus. The authors surmise that this insect-derived peptide may facilitate endocytosis by interacting with cell surface somatostatin and galanin receptors which are highly homologous to the peptide's native target.

Protein-mediated delivery

As opposed to the "minimal" peptide sequences described above, this modification requires that the entire protein be present on the QD surface to provide the key cellular membrane recognition/interaction for subsequent endocytosis. In this case, the proteins either recognize and bind a specific receptor/marker or are alternatively constitutively taken up by cells.

EGF The Jovin group used biotinylated epidermal growth factor (EGF, MW ~6 kD) complexed with commercial streptavidin QDs to bind and activate the EGF receptor in CHO and A431 cells (see Fig. 3D) [46]. They observed that the QDs were rapidly endocytosed and they were able to monitor the subsequent internal trafficking and fusion of these same labeled endocytic vesicles. Using this approach, the authors also documented the previously unreported retrograde transport of EGF-QDs from filopodia to the cell body. In this case, the EGF ligand allows the QD conjugate to bind to its specific targeted membrane receptor, activate that receptor and exploit the bound receptors' propensity to be endocytosed upon binding. The QD then functions as a specific and stable label that allows tracking of the

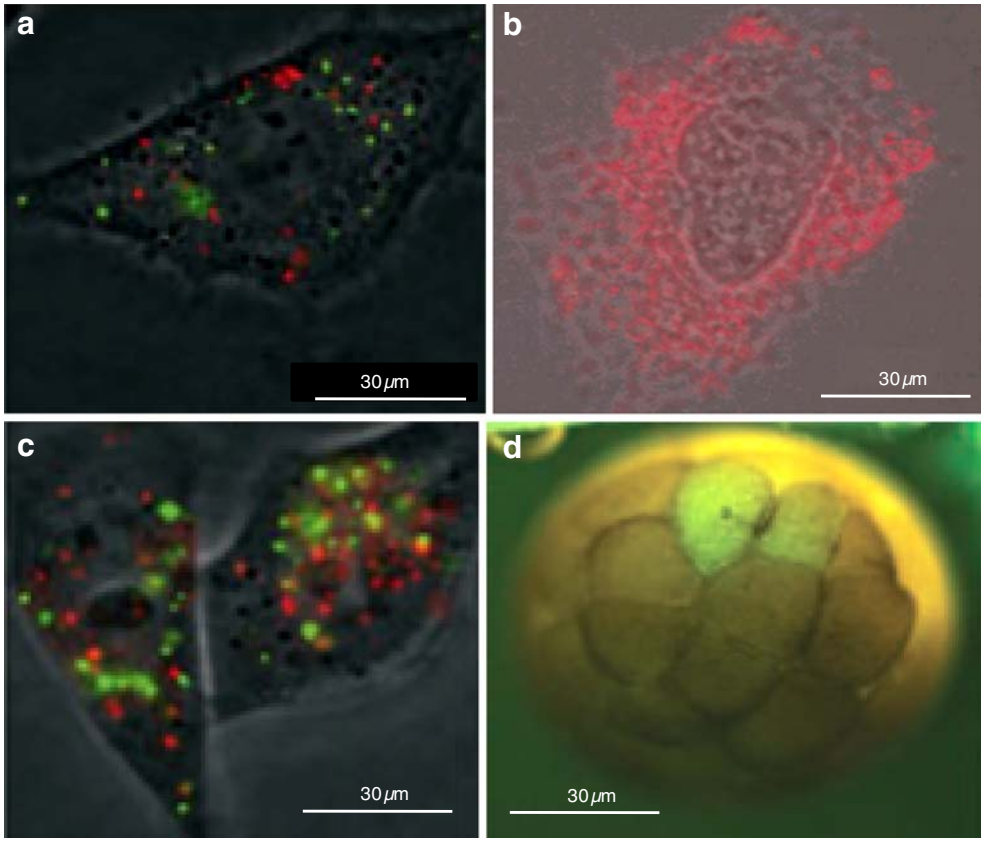

Fig. 4 Polymer-mediated and active delivery of QDs. **A** Polymer-mediated QD delivery. A HeLa cell with green-emitting PEG-coated QDs delivered via complexation with cationic liposomes. Red QDs conjugated to EGF were used as an endosomal marker. A portion of the liposome-delivered green QDs appear to have escaped from the endosomes, as seen by the slightly diffuse staining. Figure reproduced from [58] with the permission of Wiley-VCH. **B** A HeLa cell with internalized red-emitting QDs coated with a PEG-PEI copolymer demonstrating a more diffuse generalized cytoplasmic staining and outlining the nucleus. Figure reproduced from [61] with the permission of the ACS. (**C**) Electroporation. HeLa cells after electroporation of green-emitting QDs followed by incubation with red EGF-conjugated QDs (as an endosomal label). The QDs are largely outside the endosomal compartment and are present in the cytoplasm as aggregates. Figure reproduced from [58] with the permission of Wiley-VCH. **D** Microinjection. Individual QDs were encapsulated inside phospholipid block-copolymer micelles and injected into a single cell of a *Xenopus* embryo at the blastomere stage. Figure reproduced from [68] with the permission of the AAAS

internalized receptor dynamics over time. The Bawendi group utilized a family of water-soluble QDs capped with PEG-modified DHLA ligands to demonstrate labeling and tracking of the same EGF receptor but using a slightly different labeling scheme [47]. They first engineered a recombinant streptavidin protein expressing a polyhistidine terminus and capable of self-assembling via metal-affinity to the QD's surface in the same manner as we attached the TAT-peptide above [30]. By utilizing HeLa cells preincubated with biotinylated EGF, they were able to complex the self-assembled streptavidin–QD conjugates to the targeted receptor on the cell membrane and then monitor receptor trafficking in real time. Diagaradjane and coworkers took this same QD–protein combination a step further and demonstrated that near-IR emitting QDs functionalized with EGF could enhance tumor contrast in a mouse model system four hours after administration [48]. EGF receptor expression is upregulated in many different tumor types and is considered a therapeutic target. This exciting result represents the first pharmacokinetic characterization of a robust EGF receptor imaging probe and may potentially allow continuous monitoring and correlation of receptor expression levels with tumor progression in vivo.

Transferrin Transferrin (MW 75–80 kD) is a serum glycoprotein that tightly binds and carries iron and it is actively endocytosed after binding to the transferrin receptor, making transferrin both a convenient intracellular delivery agent for various cargoes and a specific marker for endosomal staining. The decrease in endocytic pH allows the protein to release iron, and it is later transported through the endocytic cycle back to the cell surface (recycled) for another round of iron transport. This well-understood system actually formed the basis for one of the first biological demonstrations of quantum dots, when Chan and Nie coupled transferrin to mercaptoacetic acid-capped

QDs using carbodiimide (EDC) chemistry and demonstrated specific cellular uptake and endosomal delivery of the nanocrystals [49]. Use of transferrin to facilitate QD delivery is still popular [50–53], and has even been used to deliver QDs to different strains of bacteria [54].

Antibodies Another robust way to deliver QDs into cells is to decorate the QDs with an antibody (MW ~150–200 kD) directed against a specific cell surface protein that is actively endocytosed. Using this approach, Qian and coworkers labeled and imaged pancreatic cancer cells with QDs conjugated to an anti-Claudin-4 antibody. The specificity in labeling just these cells results from the Claudin-4 membrane protein being preferentially upregulated in these cancer cells [51]. In another example, Zhang et al. coupled an anti-type I insulin-like growth factor receptor (IGF1R) antibody to commercial QDs by using a heterobifunctional linker that joined amine groups on the QD to thiols on the antibody [55]. The QD immunoconjugate was then applied to both detect and measure IGF1R levels in breast cancer cells (MCF−7 cells). The authors also noted that after the QDs were internalized by endocytosis of the receptor, they appeared to become more perinuclear, with some QDs colocalizing with the DAPI-stained nuclei over time. This last system has direct clinical relevance, as several monoclonal antibodies directed against IGF1R are currently in clinical trials and determining their binding efficacy and therapeutic outcome will be critical. Similar to the EGF system described above, these conjugates utilize the antibody–cell membrane marker specificity for recognition and also exploit endocytosis of the bound receptor for delivery. The use of antibodies is particular appealing, as it can allow specific targeting of cancer cells that (over)express a unique membrane marker in vivo.

Cholera toxin B Cholera toxin B (CTB) is the nontoxic cell-binding subunit of cholera toxin that binds to ganglioside receptors present on the surfaces of nearly all mammalian cells, and it has been used to facilitate the intracellular delivery of numerous other types of materials [56]. Chakraborty et al. covalently attached CTB to QDs and observed the conjugates to be efficiently internalized by NIH3T3 cells. This resulted in a staining pattern dispersed throughout the cytoplasm within small vesicles. In comparison, labeling of the same cell line with commercially available QTracker^{TM} QD–polyarginine conjugates rapidly resulted in what appeared to be staining and sequestration within large perinuclear endosomes.

Polymer-mediated delivery

In this strategy, the polymers (usually lipids) surround the QDs (either individually or more commonly as aggregates) and facilitate cellular uptake of the QDs. The amphiphilic nature of many of these reagents provides both aqueous compatibility to the conjugate and the ability to interact with and cross the highly hydrophobic lipid membranes. Polymer endgroups can also function as sites for further chemical modification with targeting ligands.

Lipid-based polymer Schroeder prepared water-compatible ~100 nm polymeric nanoparticles containing QDs by entrapping hydrophobic as-synthesized core-only QDs into phospholipid micelles [57]. A large portion of the phospholipid layer of the resulting “lipodots” was comprised of polyethylene glycol-distearoyl-phosphatidyl ethanolamine (mPEG-DSPE) to increase the potential in vivo circulation time of the particles by decreasing the clearance rate of the reticuloendothelial system. The incorporation of folate through the addition of folate-modified (see below on folate) mPEG-DSPE after micelle encapsulation aided in the specific targeting of the particles to mouse J6456 lymphoma cells and human head and neck KB cancer cells. Both of these cell types are known for their upregulated expression of folate receptors. The authors also found that both binding and internalization of the lipodot could be inhibited by adding free folate, while no uptake was found in a folate-receptor-negative cell line. Similar to some of the studies utilizing EGF-modified QDs discussed previously, the authors were able to extend their research to an in vivo model and demonstrated selective binding and uptake of folate-targeted lipodots by J6456-FR cells in vivo after intra-peritoneal injection in mice bearing ascitic J6456-FR tumors. In a well-known study comparing some intracellular QD delivery strategies, Derfus and coworkers used the commercial cationic liposomal reagent Lipofectamine 2000 to mediate electrostatic assembly with negatively charged QDs; see Fig. 4A [58]. Although used primarily for the transfection of plasmid DNA, the resulting liposomes still provided a high efficiency of intracellular delivery via endocytosis to HeLa cells. The authors also observed that a portion of the internalized QD materials subsequently appeared to escape from endosomes and access the cytoplasm. Unfortunately, once escaped, the QDs formed aggregates several hundred nanometers in diameter.

As an alternative to the transfection agents, micelle encapsulation or the formation of bilayer vesicles with entrapped QDs can also be utilized. Examples include the use of spontaneously formed phospholiposomes [59] and zwitterionically driven formation of lipid quantum-dot bilayer vesicles [60]. This approach offers the possibility of entrapping hydrophilic QDs in a central aqueous pocket or organic-functionalized hydrophobic QDs in the lipid bilayer. The lipids utilized can also be chosen to have a propensity to fuse with cellular membranes. Indeed, Gopalakrishnan and coworkers utilized the latter two

properties to deliver hydrophilic QDs to the cytoplasm or hydrophobic QDs to the cell membrane, allowing the specific labeling of either compartment [59]. However, the lack of control over the relative QD concentration, the numerous preparatory steps and, more importantly, the far larger sizes of the final QD-conjugate/vesicle, which can range from 50 nm to 50 μm in size, may not make this approach widely desirable or utile for many applications.

Polyethyleneimine Nie's group used QDs grafted with PEG and the endosome-disrupting polymer polyethyleneimine (PEI) fused together as a hyperbranched copolymer to deliver QDs to HeLa cells via endocytosis; Fig. 4B [61]. These conjugates then exploited PEI's "proton-sponge effect" (an endosmolytic effect mediated by the large number of amines present on PEI) to subsequently cause disruption of the acidic endosome and release QDs into the cytoplasm [61]. They observed that grafting the copolymer with more PEI-PEGs dramatically improved the rate of release. Using several counterstains specific for different intracellular compartments and organelles, they also noted that the intracellular distribution was very different from that of peptide-delivered QDs. The incorporation of the polyethylene glycol into the PEI was cited as the mitigating reason for partially reducing the otherwise highly cytotoxic effects of PEI.

Small molecules

A variety of small biologically relevant molecules, such as nutrients or cofactors, can also be used to functionalize the QD surface and, similar to the protein/peptide examples above, provide the key initial interaction with a targeted receptor for endocytic uptake.

Glucose de Faries utilized CdTe/CdS QDs capped with mercaptoacetic acid and noncovalently complexed with glucose to monitor the kinetics of glucose uptake activity into living Baker's yeast cells (*Saccharomyces cerevisiae*) [62]. Glucose is the preferred carbon source for yeast, which constitutively expresses several high-affinity glucose transporters at the cell membrane. The QD-complexed glucose allowed the QDs to interact with this transport system and undergo facilitated transport, yielding what appeared to be highly efficient, diffuse staining of the cytoplasm after short (<10 min) incubations. Although only an initial experiment, this result is interesting as it suggests the possibility that the QD–sugar complexes could be actively transported through the membrane by an integral membrane transport protein and thus bypass endocytosis. This transport occurs even though glucose (MW 180.2), the preferred substrate of this symporter family of transmembrane proteins, is orders of magnitude smaller than the far larger QD. It is possible that nuclear pore proteins may use a similar type of process to transport NLS-conjugated QDs into the nucleus.

Folate Folic acid is the water-soluble form of vitamin B9 and is a required cofactor for a number of essential biosynthetic pathways, such as DNA synthesis. Prasad's group coupled InP-ZnS QDs capped with mercaptoacetic acid to folic acid using modified carbodiimide chemistry [63]. They demonstrated high levels of receptor-mediated endocytic uptake in a human folate receptor expressing nasopharyngeal epidermal carcinoma KB cell line and a far lower delivery efficiency to the non-receptor human lung carcinoma A549 cell line. They also noted accumulation of the QDs in islands of multivesicular bodies (endosomal intermediaries) near the nucleus after 3 h.

In examining all of these QD delivery schemes cumulatively, several common properties emerge. All of the modifications discussed above share in common the addition of a functional, targeting moiety to the QD surface to form a QD bioconjugate that can be readily internalized by the cellular machinery in disparate cells, ranging from bacteria and yeast to a wide variety of eukaryotic cells (see Table 3). There is a distribution among these approaches in terms of the ease of bioconjugate formation, the resulting bioconjugate size, and in some cases the ultimate intracellular fate. Noncovalent assembly is clearly the most facile means of bioconjugate formation, and it further benefits from obviating the need to separate the unreacted targeting molecules from the QDs (in most cases) prior to incubation of the conjugates with cells. The use of peptides and then proteins also yields assemblies that are smaller in overall size (~5–20 nm in diameter) than conjugates formed with cationic polymers and liposomes, which can be as large as several 100 nm in diameter. It is also worth mentioning that because of their small size, peptide- and protein-derived conjugates offer promise for the development of FRET-based intracellular sensors where the distance between the QD donor and a proximal dye acceptor must be minimized [9]. As an alternative, commercial polymeric transfection reagents are already well accepted for DNA delivery; however, they contain proprietary materials and thus not all components will be known to the user. It is also understood that these reagents require empirical optimization for each cell line used.

Several examples have shown that decorating the QDs with a specific ligand can significantly enhance delivery to a targeted cell type, which suggests exciting possibilities for in vivo delivery to targeted tumors, many of which are known to express upregulated receptors on their surface. Overall, the use of peptides may be the most utile approach for QD delivery. The advantages of this strategy include

demonstrated noncovalent conjugation (i.e., biotin–avidin or histidine self-assembly), the small size of the resulting conjugate, short incubation times, minimal toxicity, and overall loading efficiency. Furthermore, different sequences can be utilized at controlled valences with QDs exhibiting a variety of surface coatings. Indeed, a commercial product, the QTracker™ kit from Invitrogen, uses a polyarginine peptide for generalized QD cellular delivery.

As endocytosis is the primary mechanism of uptake, it is not surprising to find most of the facilitated delivery strategies result in endosomal sequestration of the QD conjugates. For generalized cellular labeling and tracking experiments this may be sufficient. However, progressing to sensing intracellular processes will require access to the cytoplasm and to specific organelles. Furthermore, endosomes are highly acidic in nature, which may degrade the QD conjugates over time. Although some reports suggest QD uptake and cellular staining that reflects endocytic escape, these appear to be confined to a particular cell line and need to be more thoroughly confirmed with appropriate counterstaining techniques. To date, endosomal escape strategies, such as addition of free PEI, have yielded mixed results, and success appears to vary depending on the cell type being targeted [64, 65]. More general endosomal escape strategies need to be developed in order for facilitated delivery to reach its full potential across a wider variety of cell types. Another important issue that is not commonly mentioned is that of intracellular precipitation of the QD materials themselves, which would preclude any further intracellular sensing. This probably originates through a combination of confinement in the acidic endosome and the choice of the QD capping ligand used. This issue can be rectified through the development of improved, more robust surface-capping ligand chemistry.

Active delivery

In comparison to facilitated delivery, which takes advantage of the inherent cellular uptake machinery, active delivery involves direct physical manipulation of the cell and encompasses the techniques of electroporation and microinjection. A third active method is scrape-loading of adherent cells; however, its crude nature involves severe damage to the cellular structure, high mortality; as it is generally falling out of favor it will not be discussed here.

Electroporation This method uses an electrical pulse to temporarily permeabilize the phospholipid bilayer of the plasma membrane. It is commonly used to transfect DNA into a variety of different cell types, and it has also been used by a number of groups to deliver QDs into cells. The Bhatia group used electroporation to deliver monothiolated PEG-modified CdSe/ZnS QDs into HeLa cells; see Fig. 4C [58]. While the delivery was highly efficient, the nanoparticles formed aggregates up to 500 nm in diameter within the cytoplasm. Crosslinking the QDs to the commonly used carrier protein bovine serum albumin (BSA) prior to electroporation did not help to ameliorate the intracellular aggregation. The fact that the same type of QDs could be effectively delivered using peptide-mediated delivery and lipid transfection reagent strongly suggests that electrical pulse/field effects on the QD dispersion was the source of the problem. The group of Chen and Gerion coupled electroporation to peptide targeting and delivered QDs bearing a nuclear-localization peptide into HeLa cells via electroporation [66]. Streptavidin-conjugated silanized QDs emitting at ~550 nm were pre-assembled with biotinylated peptides expressing the SV40 large T-antigen NLS, and they observed both perinuclear and nuclear localization of the QD complexes 24 h after electroporation. Control experiments with QDs bearing an irrelevant control peptide sequence did not show this behavior, helping to confirm the specificity of delivery.

Slotkin and coworkers electroporated commercial phospholipid CdSe/ZnS QDs into developing mouse neural stem and progenitor cells (NSPCs) at the two-cell embryo stage [67]. They were able to show that the labeled cells were compatible with early embryonic development in vitro and were able to extend the labeling to in utero cells using an ultrasound-guided electroporation system they developed in-house. They found that the QD-labeled NSPCs continued to develop, migrate, and differentiate normally throughout the development process. This proof-of-principle study also serves as a good example of why there is such strong interest in these materials. It demonstrates that QDs can be used to label cells at a very early developmental stage and that the long-term photo/chemicostability can then be exploited for in vivo fate mapping along with monitoring migration and differentiation—something that is very hard to achieve with currently available conventional organic dyes.

Microinjection Microinjection allows delivery of very small sample volumes (usually femtoliters) directly into the cytoplasm of individual cells. It uses a fine-tipped glass microcapillary combined with a fluorescent microscope to guide the targeting of the cells. In contrast to all of the other techniques described above, this is the only technique where the target cell is directly visualized first. In one of the first examples that utilized this technique for QD delivery, Dubertret et al. microinjected QDs encapsulated within phospholipid block-copolymer micelles into Xenopus embryo cells at the blastomere stage; see Fig. 4D [68]. The embryos were then imaged over time at various stages of development and followed to the tadpole stage. They estimated remarkable initial loadings of 2.1 to 4.2×10^9

injected nanoparticles per cell, and observed that the QD-loaded micelles partitioned amongst daughter cells within the growing embryo. Similar to points made for the Slotkin experiment described above, direct loading of a targeted cell in an embryo allowed lineage-tracing experiments that monitored long-term embryogenesis. Derfus et al. also microinjected PEG-functionalized QDs into the cytoplasm of HeLa cells and found that the QDs were monodisperse, producing a diffuse staining of the entire cell interior [58]. When QDs bearing an NLS peptide were injected, the authors observed what appeared to be the active transport and selective nuclear accumulation of the QDs within the nuclei of the majority of cells. This is similar to the results reported by Chen and Gerion above when they electroporated QD-NLS conjugates into the same cell line.

In examining these two active delivery methods, we see that electroporation is well suited for QD delivery to large numbers (often ~10^6) of either adherent or nonadherent cells simultaneously, as the electrical pulse can be delivered to controlled densities of suspended cells when they are coincubated with QDs. Modifications of this technique have also been recently developed for addressing adherent cells directly without having to trypsinize/resuspend them, although this has not yet been reported for QD delivery. As this technique bypasses the endocytic pathway, the QD materials are delivered directly to the cytoplasm with no need for subsequent endosomal escape, which is clearly another benefit. However, as the cells are both permeabilized and subjected to a very strong electrical pulse, there is usually a high rate of cellular mortality which is not often reported. Intracellular aggregation of the electroporated nanoparticles also remains an issue [58]. In comparison, microinjection delivers the QDs directly to the cytoplasm and seems to induce a lower rate of cell death. It is, however, very limited in its throughput, as each cell needs be individually selected/visualized and then injected. This serial technique is geared towards the manipulation of tens to hundreds of cells at a time, and also requires a well-trained operator. Furthermore, not all cells in a field of view will be successfully microinjected due to physical constraints, including cell morphology, membrane thickness, cell height, etc. From a practical standpoint, microinjection devices are also very expensive (~$30–40,000) relative to electroporation devices (<$5,000). In comparing the images in Figs. 2C and 4D, where microinjection was employed, to those collected using other methods (Figs. 2, 3, 4), the allure and pinpoint efficiency of this technique become clearly visible.

Remaining issues and outlook

It is clear that as biocompatible QDs are developed they will make powerful basic cellular probes and research tools. Their unique photophysical properties already complement conventional organic and protein-based fluorophores in cell biology. As the complex nanoscale platforms for in vivo sensing or targeted drug delivery vehicles become a reality, we can expect much of the technical engineering to employ luminescent QDs. Indeed, preliminary examples are already appearing and include peptide-modified QDs that only undergo endocytosis after extracellular protease activation [69] or bioluminescent QD–enzyme conjugates that can self-illuminate in vivo [70]. However, in order to accomplish any of these postulated roles, the QDs must be able to undergo controlled delivery to any cell or tissue.

The reports reviewed here indicate that, overall, intracellular delivery of QDs/QD bioconjugates is strongly affected by the nature of both the QD conjugate itself and the cell types utilized. Much basic work on engineering the QD surfaces and creating QD bioconjugates with control over all relevant properties remains to be done. Ideally, when designing a QD bioconjugate, one would like to control the number of biomolecules attached per QD (valence), their orientation, their distance from the QD surface, and the strength of their attachment [71]. Unfortunately, the currently available QD surface functionalization strategies in combination with the available bioconjugation chemistries cannot provide this in all cases. Each conjugation strategy has its own set of benefits and liabilities, and thus what may work for one conjugation method cannot automatically be applied to another [2]. For example, use of the common biotin–avidin linkage necessitates biotinylating the biomolecule(s) of interest and working with the cognate avidin-coated nanocrystals. In the case of biotinylated antibodies or other proteins, this can lead to heterogeneous attachment and mixed avidity, since the biotin targets the multiple lysine residues that are ubiquitously present on each molecule. Overbiotinylation or mixing of nonoptimal ratios can also result in crosslinking and precipitation of streptavidin-functionalized QDs [2]. Many researchers commonly utilize monothiolated/carboxylated ligands as surface caps, and these tend to have a strongly dynamic off-rate and are confined to basic pH, giving the hydrophilic QD a short useable half-life combined with limited applicability. Alternatives include dithiol-PEGylated ligands, which have already been shown to provide better long-term pH stability [13].

Conjugate size is also another crucial aspect. Although the QDs can have “hard” sizes (core–shell) comparable to that of a large protein (Table 1), it is important to note that the surface-functionalization and further conjugation of biomolecules can increase the QD bioconjugate size and hydrodynamic size substantially. For example, the hydrodynamic radius of similarly emissive hydrophilic CdSe-ZnS QDs can vary from ~5 nm (for nanocrystals cap-exchanged with molecular ligands) to >20 nm (for nanocrystals

encapsulated within block copolymers) [72]. Such large sizes may limit access to intracellular organelles and alter the intrinsic activity of any attached proteins. Thus, developing surface functionalization techniques that maintain a small overall size is highly desirable.

Cellular physiology is another area not often discussed in these reports. As with most other biological research, the most common cells utilized are transformed or tumor cell lines, which can be directly relevant to tumor targeting studies. However, the dedifferentiated (abnormal) state of these cells in conjunction with their altered properties (for example over-expression of particular receptors or differing average chromosomal counts) means that the uptake results and observed fates must always be examined with this context in mind. The toxicity of the QD materials themselves also appears to be a constant source of concern [73, 74]. This can arise from both the nanoscale size of the material and the semiconductor metals in the core–shell structure [33, 75]. More pertinently, when evaluating nanotoxicity it appears that the use of many different QD materials and surface preparations at different concentrations in many different cell lines have given rise to disparate results and conclusions. Some experts in the area of nanotoxicity have already suggested that these types of "piecemeal" studies may not be meaningful in the absence of adequate material characterization and without a full understanding of the nature of the cells used [76, 77]. For example, Tekle and coworkers performed colocalization studies in HeLa cells with QD–streptavidin–transferrin conjugates, and concluded that the QDs induced changes in normal endocytic vesicle routing which "may have severe consequences on cell physiology" [78]. It is worth noting that they measured the hydrodynamic diameter of their transferrin–QD bioconjugates to be a rather large ~50 nm, utilized only commercial QD preparations, and their observations were only made in one cell line after fixation—a process which has been reported to alter endocytic staining [78, 79]. Further, it is not clear whether it is just the size of the conjugate that is problematic, which could be remedied by using far smaller conjugates [72]. In contrast, Lidke showed that when similar streptavidin QDs were functionalized with a different protein ligand (EGF, discussed above), the bioconjugate was endocytosed and even underwent retrograde transport normally in a different cell line (A431 cells) [46]. Despite these kinds of contradictory results, a consensus is slowly growing that the major determinants for QD cytotoxicity are the inherent constituents of the core (CdSe vs. CdTe), the physical nature of the QD (core vs. core–shell), and the surface-functionalizing ligands utilized, and careful engineering can mitigate most overt problems [33, 66, 80]. As with most complex problems, full and comprehensive studies where all relevant parameters are explored are needed before a final conclusion can be drawn.

In summary, we see that much has been accomplished to develop methods for the controlled delivery of QDs to cells, and much has been learned in the process. However, this is only the initial phase, and even more remains to be done. Progress in this area will have important implications for not only QDs but also a variety of other biocompatible nanoparticles, and help propel the growing field of bionanotechnology forward. From just the lessons learned to date, we can expect that advanced QD-based sensors will begin preliminary testing in both cell culture and animal models in the near future.

Acknowledgements The authors acknowledge Jennifer Becker and Ilya Elashvilli of the CB Directorate/Physical S&T Division (ARO/DTRA), ONR, NRL, and the NRL-NSI for financial support.

References

1. Murray CB, Kagan CR, Bawendi MG (2000) Ann Rev Mater Sci 30:545–610
2. Medintz I, Uyeda H, Goldman E, Mattoussi H (2005) Nature Mater 4:435–446
3. Michalet X, Pinaud FF, Bentolila LA, Tsay JM, Doose S, Li JJ, Sundaresan G, Wu AM, Gambhir SS, Weiss S (2005) Science 307:538–544
4. Alivisatos AP, Gu W, Larabell CA (2005) Ann Rev Biomed Eng 7:55–76
5. Alivisatos AP (2004) Nature Biotech 22:47–52
6. Klostranec JM, Chan WCW (2006) Adv Mater 18:1953–1964
7. Larson DR, Zipfel WR, Williams RM, Clark SW, Bruchez MP, Wise FW, Webb WW (2003) Science 300:1434–1437
8. Clapp AR, Pons T, Medintz IL, Delehanty JB, Melinger JS, Tiefenbrunn T, Dawson PE, Fisher BR, O'Rourke B, Mattoussi H (2007) Adv Mater 19:1921–1926
9. Clapp AR, Medintz IL, Mattoussi H (2005) ChemPhysChem 7:47–57
10. Medintz IL, Clapp AR, Brunel FM, Tiefenbrunn T, Uyeda HT, Chang EL, Deschamps JR, Dawson PE, Mattoussi H (2006) Nature Mater 5:581–589
11. Medintz IL, Clapp AR, Mattoussi H, Goldman ER, Fisher B, Mauro JM (2003) Nature Mater 2:630–638
12. Goldman ER, Medintz IL, Whitley J, Hayhurst A, Clapp AR, Uyeda HT, Deschamps JR, Lassman M, Mattoussi H (2005) J Am Chem Soc 127:6744–6751
13. Susumu K, Uyeda HT, Medintz IL, Pons T, Delehanty JB, Mattoussi H (2007) J Am Chem Soc 129:13987–13996
14. Pinaud F, King D, Moore HP, Weiss S (2004) J Am Chem Soc 126:6115–6123
15. Sapsford KE, Pons T, Medintz IL, Higashiya S, Brunel FM, Dawson PE, Mattoussi H (2007) J Phys Chem C 111:11528–11538
16. Wu X, Liu H, Liu J, Haley KN, Treadway JA, Larson JP, Ge N, Peale F, Bruchez MP (2003) Nature Biotech 21:41–46
17. Howarth M, Takao K, Hayashi Y, Ting A (2005) Proc Natl Acad Sci USA 102:7583–7588
18. Chattopadhyay PK, Price DA, Harper TF, Betts MR, Yu J, Gostick E, Perfetto SP, Goepfert P, Koup RA, De Rosa SC, Bruchez MP, Roederer M (2006) Nature Med 12:972–977

19. Luccardini C, Yakovlev A, Gaillard S, van't Hoff M, Alberola AP, Mallet JM, Parak WJ, Feltz A, Oheim M (2007) J Biomed Biotechnol 2007(7):68963
20. Ozkan M (2004) Drug Discov Today 9:1065–1071
21. Emerich DF, Thanos CG (2006) Biomol Eng 23:171–184
22. Hild WA, Breunig M, Goepferich A (2008) Eur J Pharm Biopharm 68:153–168
23. Sukhorukov GB, Mohwald H (2007) Trends Biotechnol 25:93–98
24. Jiang W, Kim BYS, Rutka JT, Chan WCW (2007) Exp Opin Drug Deliv 4:621–633
25. Kim S, Lim YT, Soltesz EG, De Grand AM, Lee J, Nakayama A, Parker JA, Mihaljevic T, Laurence RG, Dor DM, Cohn LH, Bawendi MG, Frangioni JV (2004) Nature Biotech 22:93–97
26. Groman EV, Bouchard JC, Reinhardt CP, Vaccaro DE (2007) Bioconjug Chem 18:1763–1771
27. Bakalova R, Zhelev Z, Aoki I, Kanno I (2007) Nature Photonics 1:487–489
28. Watson P, Jones AT, Stephens DJ (2005) Adv Drug Deliv Rev 57:43–61
29. Jaiswal JK, Mattoussi H, Mauro JM, Simon SM (2003) Nature Biotech 21:47–51
30. Delehanty JB, Medintz IL, Pons T, Brunel FM, Dawson PE, Mattoussi H (2006) Bioconjug Chem 17:920–927
31. Helmick L, Antúnez de Mayolo A, Zhang Y, Cheng CM, Watkins SC, Wu C, LeDuc PR (2008) Nano Lett 8:1303–1308
32. Nabiev I, Mitchell S, Davies A, Williams Y, Kelleher D, Moore R, Gun'ko YK, Byrne S, Rakovich YP, Donegan JF, Sukhanova A, Conroy J, Cottell D, Gaponik N, Rogach A, Volkov Y (2007) Nano Lett 7:3452–3461
33. Hardman R (2006) Environ Health Perspect 114:165–172
34. El-Andaloussi S, Holm T, Langel U (2005) Curr Pharm Des 11:3597–3611
35. Frankel AD, Pabo CO (1988) Cell 1988:1189–1193
36. Ruan G, Agrawal A, Marcus AI, Nie S (2007) J Am Chem Soc 129:14759–14766
37. Lei Y, Tang H, Yao L, Yu R, Feng M, Zou B (2008) Bioconjug Chem 19:421–427
38. Santra S, Yang H, Holloway PH, Stanley JT, Mericle RA (2005) J Am Chem Soc 127:1656–1657
39. Santra S, Yang H, Stanley JT, Holloway PH, Moudgil BM, Walter G, Mericle RA (2005) Chem Commun 25:3144–3146
40. Xue FL, Chen JY, Guo J, Wang CC, Yang WL, Wang PN, Lu DR (2007) J Fluoresc 17:149–154
41. Munoz-Morris MA, Heitz F, Divita G, Morris MC (2007) Biochem Biophys Res Commun 355:877–882
42. Rozenzhak SM, Kadakia MP, Caserta TM, Westbrook TR, Stone MO, Naik RR (2007) Chem Commun 17:2217–2219
43. Lieleg O, Lopez-Garcia M, Semmrich C, Auernheimer J, Kessler H, Bausch AR (2007) Small 3:1560–1565
44. Smith BR, Cheng Z, De A, Koh AL, Sinclair R, Gambhir SS (2008) Nano Lett 8(9):2599–2606
45. Biju V, Muraleedharan D, Nakayama K, Shinohara Y, Itoh T, Baba Y, Ishikawa M (2007) Langmuir 23:10254–10261
46. Lidke DS, Nagy P, Heintzmann R, Arndt-Jovin DJ, Post JN, Grecco HE, Jares-Erijman EA, Jovin TM (2004) Nat Biotechnol 22:198–203
47. Liu W, Howarth M, Greytak AB, Zheng Y, Nocera DG, Ting AY, Bawendi MG (2008) J Am Chem Soc 130:1274–1284
48. Diagaradjane P, Orenstein-Cardona JM, E Colon-Casasnovas N, Deorukhkar A, Shentu S, Kuno N, Schwartz DL, Gelovani JG, Krishnan S (2008) Clin Cancer Res 14:731–741
49. Chan WCW, Nie S (1998) Science 281:2016–2018
50. Pan YL, Cai JY, Qin L, Wang H (2006) Acta Biochim Biophys Sin 38:646–652
51. Qian J, Yong KT, Roy I, Ohulchanskyy TY, Bergey EJ, Lee HH, Tramposch KM, He S, Maitra A, Prasad PN (2008) J Phys Chem B 111:6969–6972
52. Yong KT, Qian J, Roy I, Lee HH, Bergey EJ, Tramposch KM, He S, Swihart MT, Maitra A, Prasad PN (2007) Nano Lett 7:761–765
53. Zheng J, Ghazani AA, Song Q, Mardyani S, Chan WCW, Wang C (2006) Lab Hematol 12:94–98
54. Kloepfer JA, Mielke RE, Wong MS, Nealson KH, Stucky G, Nadeau JL (2003) Appl Environ Microbiol 69:4205–4213
55. Zhang H, Sachdev D, Wang C, Hubel A, Gaillard-Kelly M, Yee D (2008) Breast Cancer Res Treat (in press)
56. Chakraborty SK, Fitzpatrick JA, Phillippi JA, Andreko S, Waggoner AS, Bruchez MP, Ballou B (2007) Nano Lett 7:2618–2626
57. Schroeder JE, Shweky I, Shmeeda H, Banin U, Gabizon A (2007) J Control Release 124:28–34
58. Derfus AM, Chan WCW, Bhatia SN (2004) Adv Mater 16:961–966
59. Gopalakrishnan G, Danelon C, Izewska P, Prummer M, Bolinger PY, Geissbuhler I, Demurtas D, Dubochet J, Vogel H (2006) Angew Chem Int Ed 45:5478–5483
60. Al-Jamal WT, Al-Jamal KT, Tian B, Lacerda L, Bornans PH, Frederik PM, Kostarelos K (2008) ACS Nano 2:408–418
61. Duan H, Nie S (2007) J Am Chem Soc 129:3333–3338
62. de Farias PMA, Santos BS, Menezes FD, Brasil Jr AG, Ferreira R, Motta MA, Castro-Neto AG, Vieira AAS, Silva DCN, Fontes A, Cesar CL (2007) Appl Phys A 89:957–961
63. Bharali DJ, Lucey DW, Jayakumar H, Pudavar HE, Prasad PN (2005) J Am Chem Soc 127:11364–11371
64. Ciofani G, Raffa V, Menciass A, Cuschieri A (2008) Biotechnol Bioeng 101:850–858
65. Hess GT, Humphries WH, Fay NC, Payne CK (2007) Biochim Biophys Acta 1773:1583–1588
66. Chen FQ, Gerion D (2004) Nano Lett 4:1827–1832
67. Slotkin JR, Chakrabarti L, Dai HN, Carney RS, Hirata T, Bregman BS, Gallicano GI, Corbin JG, Haydar TF (2007) Dev Dyn 236:3393–3401
68. Dubertret B, Skourides P, Norris DJ, Noireaux V, Brivanlou AH, Libchaber A (2002) Science 298:1759–62
69. Zhang Y, So MK, Rao JH (2006) Nano Lett 6:1988–1992
70. So MK, Xu CJ, Loening AM, Gambhir SS, Rao JH (2006) Nat Biotechnol 24:339–343
71. Medintz IL (2006) Nature Mater 5:842
72. Pons T, Uyeda HT, Medintz IL, Mattoussi H (2006) J Phys Chem B 110:20308–20316
73. Colvin VL (2003) Nature Biotech 21:1166–1170
74. Cho SJ, Maysinger D, Jain M, Roder B, Hackbarth S, Winnik FM (2007) Langmuir 23:1974–1980
75. Nel A, Xia T, Madler L, Li N (2006) Science 311:622–627
76. Warheit DB (2008) Toxicol Sci 101:183–185
77. Hood E (2004) Environ Health Perspect 112:A740–A749
78. Tekle C, van Deurs B, Sandvig K, Iversen TG (2008) Nano Lett 8:1858–1865
79. Richard JP, Melikov K, Vives E, Ramos C, Verbeure B, Gait MJ, Chernomordik LV, Lebleu B (2003) J Biol Chem 278: 585–590
80. Derfus AM, Chan WCW, Bhatia SN (2004) Nano Lett 4:11–18
81. Murray CB, Norris DJ, Bawendi MG (1993) J Am Chem Soc 115:8706–1875
82. Medintz IL, Pons T, Delehanty JB, Susumu K, Brunel FM, Dawson PE, Mattoussi H (2008) Bioconjug Chem 19:1785–1795
83. Mok H, Park JW, Park TG (2008) Bioconjug Chem 19:797–801
84. Silver J, Ou W (2005) Nano Lett 5:1445–1449
85. Toita S, Hasegawa U, Koga H, Sekiya I, Muneta T, Akiyoshi K (2008) J Nanosci Nanotechnol 8:2279–2285
86. Jaiswal JK, Goldman ER, Mattoussi H, Simon SM (2004) Nature Methods 1:73–78
87. Rajan SS, Vu TQ (2006) Nano Lett 6:2049–2059

88. Rajan SS, Liu HY, Vu TQ (2008) ACS Nano 2:1153–1166
89. Dudu V, Ramcharan M, Gilchrist ML, Holland EC, Vazquez M (2008) J Nanosci Nanotechnol 8:2293–2300
90. Voura EB, Jaiswal JK, Mattoussi H, Simon SM (2004) Nature Med 10:993–998
91. Hasegawa U, Nomura SM, Kaul SC, Hirano T, Akiyoshi K (2005) Biochem Biophys Res Commun 331:917–921
92. de la Fuente JM, Fandel M, Berry CC, Riehle M, Cronin L, Aitchison G, Curtis AS (2005) Chembiochem 6:989–991
93. Clarke S, Nadeau J, Bahcheli D, Zhang Z, Hollmann C (2005) Conf Proc IEEE Eng Med Biol Soc 1:504–507
94. Clarke SJ, Hollmann CA, Zhang ZJ, Suffern D, Bradforth SE, Dimitrijevic NM, Minarik WG, Nadeau JL (2006) Nature Mater 5:409–417
95. Mattheakis LC, Dias JM, Choi YJ, Gong J, Bruchez MP, Liu J, Wang E (2004) Anal Biochem 327:200–208
96. Akerman ME, Chan WCW, Laakkonen P, Bhatia SN, Ruoslahti E (2002) Proc Natl Acad Sci USA 99:12617–1262
97. Stroh M, Zimmer JP, Duda DG, Levchenko TS, Cohen KS, Brown EB, Scadden DT, Torchilin VP, Bawendi MG, Fukumura D, Jain RK (2005) Nature Med 11:678–682
98. Pellegrino T, Parak WJ, Boudreau R, Le Gros MA, Gerion D, Alivisatos AP, Larabell CA (2002) Differentiation 71:542–548
99. Serge A, Bertaux N, Rigneault H, Marguet D (2008) Nature Methods 5:687694
100. Parak WJ, Boudreau R, Le Gros M, Gerion D, Zanchet D, Micheel CM, Williams SC, Alivisatos AP, Larabell C (2002) Adv Mater 14:882–885
101. Lewin M, Carlesso N, Tung CH, Tang XW, Cory D, Scadden DT, Weissleder R (2000) Nat Biotechnol 18:410–414
102. De la Fuente JM, Penades S (2006) Biochim Biophys Acta 1760:636–651